Available online at www.sciencedirect.com

ScienceDirect

Procedia Materials Science 8 (2015) 155 – 161

Procedia Materials Science

www.elsevier.com/locate/procedia

International Congress of Science and Technology of Metallurgy and Materials, SAM - CONAMET 2013

Surface Alterations Produced in Grinding of Austempered Ductile Iron

A.D. Sosa[a,b]* and M.D. Echeverría[a,b]

[a]*School of Engineering, Universidad Nacional de Mar del Plata, J.B. Justo 4302, Mar del Plata (B7608FDQ), Argentina.*
[b]*Metallurgy Division, INTEMA, J.B. Justo 4302, Mar del Plata (B7608FDQ), Argentina.*

Abstract

The technological advances achieved in recent decades have allowed to obtain cast parts of ductile iron with no metallurgical defects and of complex shapes and dimensions very close to the final ones. Heat treatments have enabled to obtain ADI within a wide range of mechanical properties. After properly choosing the processing variables, the most suitable combination of strength and toughness can be attained for each application. When restrictive dimensional or shape accuracy is required, a high precision machining process, such as grinding, is used. This process induces significant temperature gradients and surface plastic deformations which could affect the surface characteristics. The aim of this paper is to analyze the effects of grinding on power consumption, surface characteristics, roughness and distortion on ADI plates grade 2 and 5. The results indicate that it is possible to achieve excellent surface finishes with moderate power consumption and low residual stresses and distortions.

Selection and peer-review under responsibility of the scientific committee of SAM - CONAMET 2013

Keywords: Cast iron, ADI, grinding, surface, microstructure, roughness, distortion

* Corresponding author. Tel.: +54-0223-481-6600; fax: +54-0223-484-6601.
E-mail address: adsosa@fi.mdp.edu.ar

Selection and peer-review under responsibility of the scientific committee of SAM - CONAMET 2013
doi:10.1016/j.mspro.2015.04.059

Nomenclature

p	depth of cut
Vs	wheel speed
Vw	work speed

1. Introduction

World production of ductile iron (DI) has experienced a significant growth rate in recent times. Despite having been introduced in the market long ago, it has been under continuous development in recent decades, thereby extending its scope of application. Most DI production (in tons) worldwide is for heavy applications whose performance requirements are not high. However, it is also being used in a number of parts in which mechanical requirements and reliability are crucial attributes. Auto parts (crankshafts, suspension parts) and several industrial machine parts could be cited as examples.

Oftentimes, to achieve the specifications required, it is necessary to modify the microstructural features of DI by heat treatment. One of the heat treatments most frequently applied is austempering, which confers a wide range of mechanical properties. Austempered DI microstructure (ADI) consists in graphite nodules embedded in a metallic matrix of acicular ferrite and carbon enriched austenite. Basso and Sikora (2012) and Laino et al. (2011) developed variants of ADI in which dispersed carbides (carbidic ADI) and alotriomorphic ferrite (ADI Dual Phase) are present.

Currently ADI provides competitive advantages over other high resistant metallic alloys and/or light alloys, substituting them on several occasions. Some of the reasons why ADI is adopted are: lower production costs, total recycling and high strength/weight ratio. For instance, about 50 % less energy is used when manufacturing an ADI part than when a cast steel one is produced, and less than 80 % is needed if compared to a forged steel one. The possibility of obtaining complex shapes and dimensions close to the final ones reduces the number of machining operations needed afterwards. The specific weight of ADI is 10 % lower than that of steel, featuring a similar strength in many cases. Its strength is 3 times greater than that of the aluminum, being just 2.6 times heavier than it, as accounted for by Warda (1990).

Caldera et al. (2004) and David et al. (2004) showed that the progress achieved in several fields, including casting technology, has allowed to obtain healthy parts of thinner thickness each time, and that meet standardized thickness properties. Cases of successful implementation of thin wall parts include 4mm section suspension arms used by Peugeot-Citroen, 4mm thickness exhaust manifolds and turbo chargers developed by Wescast Industries Inc., and hollow connection rods devised in the Metallurgy Division at the INTEMA, among others.

Cast thickness reduction has led to an increment in cooling rates, and hence nodule counts have increased and as-cast microstructures become more refined. The above named changes in the microstructure have affected some materials properties, and can even change performance. Rebasa et al. (2002) postulated that rolling contact fatigue (RCF) resistance improves as nodule count does in ferritic ductile iron. Moreover, Caldera et al. (2007) indicated that DI with higher nodule count provides greater fatigue strength.

DI parts manufacturing comprises several stages, such as casting, heat treatment and machining. Each stage modifies the material features and alters its surface and subsurface properties. Characteristics such as decarburation and corrosion resistance, residual stress and surface hardening do not only depend on the material itself but also on the process variables used. Altered surface characteristics presence and amount can affect parts performance by enhancing or rendering them less suitable for a given application as underlined by ASM (1996), Rebasa et al. (2002), Massone et al. (2003) and Sosa et al. (2009)(2010).

In view of the fact that DI parts can achieve shapes and dimensions very close to the final ones, the machining operations performed are for finish purposes. Surface grinding is the most common finish machining process employed and involves abrasive chip formation, a process that produces a great amount of heat and leads to plastic deformations that modify material surface properties.

This paper aims to characterize ADI microstructure and analyze the effects of grinding applying different cutting conditions on power consumption, surface characteristics, roughness and shape distortion on thin ADI plates grade 2 and 5 (ASTM A897) and different nodule count.

2. Experimental procedure

The studied material was produced in a 50 kg medium-frequency induction furnace all at once. The melt was heated up to 1540 °C before pouring. Nodulisation was carried out using the sandwich method adding FeSiMg, and inoculation was performed with FeSi during transposing to one second ladle. The moulds were made using AFS-GFN 60 silica sand and alkyd resin as a binder, to cast thin plates of 4 mm thickness and "Y" blocks of 12.5 thickness. The chemical composition of the melt was determined by spark optical emission spectrometry on a sample cast before last mould. CQ was slightly hypereutectic: CE>4.3.

Table 1. Chemical composition.

%C	%Si	%Mn	%S	%P	%Mg	%Cu	%Ni	%Fe	CE
3,40	3,08	0,12	0,013	0,033	0,041	0,63	0,50	balance	4,43

Metallographic characterizations were conducted at different stages. Samples were cut, included and polished using conventional methods. To carry out metallographic observations, the polished surfaces were etched with nital 2 %. SEM, optical microscopy and digital analysis of images were performed.

The nodule count was determined on metallographic samples using the GNU software Image J. The nodule count was 160 nod/mm² and 530 nod/mm² for 12.5 mm and 4 mm cast thickness, respectively. Nodularity was over 90 % in all cases.

The material was cut and squared off under low energy cutting conditions. Several sets of samples were machined by mechanical shaping to dimensions of 100 x 12.5 mm.

Two heat treatments of 2 stages each were carried out in an electric furnace and a salt bath. The first stage comprised the complete austenitizing performed in a protective atmosphere. The second consisted in austempering at two different temperatures. Table 2 lists the conditions under which each treatment was conducted.

Table 2. Heat treatments.

Abbreviation	Stage 1	Stage 2
ADI280	Austenitizing at 900 ºC for 60 minutes	Austempering in salt bath at 280 ºC for 45 min
ADI360		Austempering in salt bath at 360 ºC for 45 min

After heat treatments, faces were recessed with 220 grit size SiC waterproof paper, in order to obtain flat faces and remove surface defects as well as the material affected by previous machining processes.

Straight surface grinding experiments were carried out on a peripheral surface grinder with a permanent magnetic chuck. A standard vitrified wheel identified as IC36/46I/J5V9 and a 5% aqueous solution soluble oil as cooling fluid were used. On each sample, semi-rough grinding conditions were applied, with three equal depth of cut (p) per pass and different wheel speed (Vs) and work speed (Vw) combinations, as particularized in Table 3.

Table 3. Cutting conditions employed on grinding assays.

Condition	Wheel speed Vs [m/s]	Work speed Vw [m/min]	Depth of cut p [mm]
(I) [20-28]	20	28	0.03
(II) [30-28]	30	28	0.03
(III) [30-16]	30	16	0.03

During each assay, the absorbed power was measured with a lab wattmeter. The meter was connected using both voltage and current transformers as well as a voltmeter and an ammeter to avoid damages. The peak consumption in each pass was recorded. The average effective values (subtracting free power consumption) were reported.

Phase identification and analysis were performed by x-ray diffraction (XRD). A Phillips XPERT-PRO diffractometer was utilized with graphite monochromated Cu-Kα radiation (λ = 1.5418 Å). The Powder Cell software developed by Kraus and Nolze (1998) for peak profile refinement was applied to analyze XRD patterns and obtain peak positions, full width at half maximum (FWHM) and intensities as well as austenite volume fraction (V_γ %) and its lattice parameter a_γ .

Specimen surfaces, after and before grinding assays, were measured with a coordinate measure machine with an uncertainty of (5±L/1000) μm. The three-dimensional distribution of points on both surfaces were obtained. Amplified three-dimensional graphs were plotted to determine the type and orientation of each specimen distortion. The distortion or maximum deviation in a perpendicular direction with respect to an ideal plane was established. The distortions in the ground face once the part is removed from the machine were reported.

The arithmetic mean roughness (Ra) and total roughness (Rt) determinations produced during grinding assays were obtained with a stylus profilometer (Taylor Hobson Surtronic 3+) and software Talyprof. Five to ten measurements were performed on each specimen and the average values were reported.

3. Results and discussions

3.1 Microstructures

Figure 1 illustrates the optical micrographies and SEM of samples under austenitizing and austempering heat treatment to obtain ADI. As it can be noticed, the microstructure is composed of graphite nodules embedded in an ausferritic metallic matrix. Samples austempered at 280 ºC display a more refined microstructure.

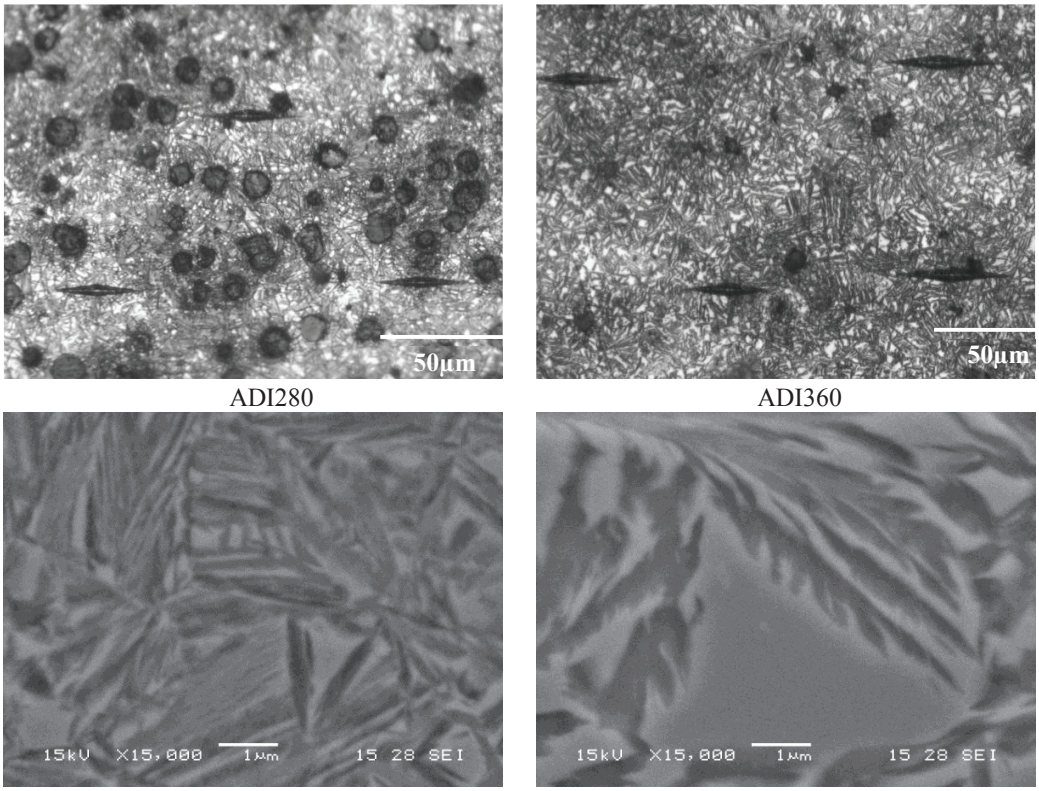

Fig. 1. Obtained microstructures. (l) ADI280, (r) ADI360

Table 2 summarizes the data collected from the characterization on heat treated samples. Materials hardness is in line with the expectations for ADI grade 2 and 5 under ASTM A897. Samples austempered at 360 ºC yielded a

larger amount of austenite, and, additionally, carbon content was slightly higher. On the other hand, full width at half maximum (FWHM) was lower, thereby denoting a lesser amount of interphases and a lower degree of crystal network distortion resulting from a less severe cooling step at quenching.

Table 4. Characteristics of heat treated samples

		ADI280	ADI360
Rockwell C Hardness	160 nod/mm^2	43 ± 1	34,5 ± 0,5
	530 nod/mm^2	45 ± 1	32 ± 1
Austenite Volume fraction %		19.5 ±2.5	27.2 ±0.1
Austenite carbon content %		0.169 ± 0.001	0.174 ± 0.003
FWHMº		0.160 ±0.001	0.135 .005

3.2 Surface roughness

Figure 2 depicts, as an example, SEM pictures from the surface of ADI360 samples with 530 nod/mm^2 grinding under condition (I). No cracks or laps nor any other defect that could arise from grinding was reported. Nonetheless crushed hollow pits in which graphite nodules are lodged near the surface were noticed. The scratch pattern obtained is in agreement with the machining type and the employed operative conditions.

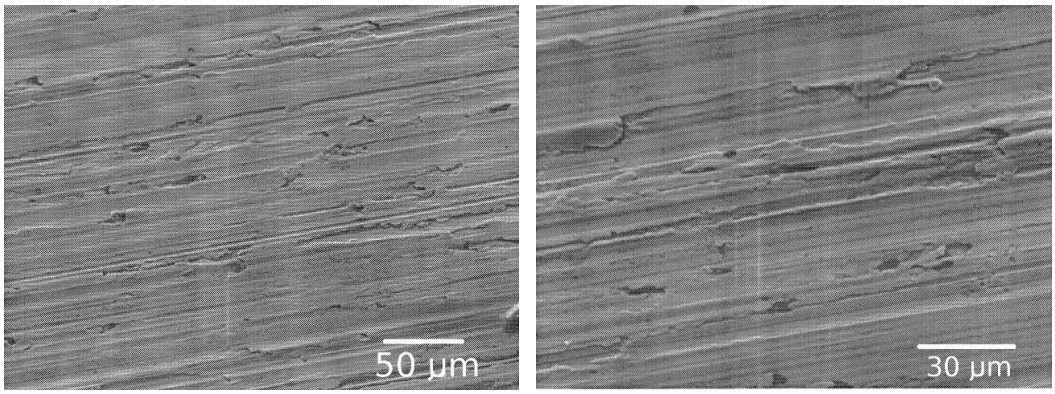

Fig. 2. Surface texture of ground ADI360 samples.

Table 5. Surface roughness of ground ADI samples.

	ADI280				ADI360			
	530 nod/mm^2		160 nod/mm^2		530 nod/mm^2		160 nod/mm^2	
Condition	Ra[µm]	Rt[µm]	Ra[µm]	Rt[µm]	Ra[µm]	Rt[µm]	Ra[µm]	Rt[µm]
(I) [20-28]	0.468	3.650	0.403	2.898	0.434	0.363	0.496	3.555
(II) [30-28]	0.525	4.427	0.514	4.648	0.479	4.450	0.487	4.122
(III) [30-16]	0.622	4.253	0.615	4.013	0.371	3.097	0.557	4.071

Table 5 provides the average roughness values calculated from ground surfaces. Even though semi-rough (p= 0.03 mm) passes were performed, surface quality was very good, reaching a maximum value of Ra= 0.622 µm. Based on data provided by Saint-Gobain abrasive wheels manufactures, for a conventional reciprocating surface grinding of medium resistance material, roughness can be expected to be within 0.8 to 1.2 µm under finish conditions. This evidences the high surface quality attained. No significant differences were obtained in regard to nodule count, though they were observed with respect to different ADIs. This can be attributed to marked difference in hardness. The highest Ra values were collected under the lowest mean undeformed chip thickness condition (III).

Under said condition, the force on the abrasive grits is very small, thus hindering their renewal, which translates into degradation of the surface quality obtained. Rt values followed the same trend as Ra values did, with values below 5 μm in all cases.

3.3 Power consumption

Figure 3 plots the effective power values consumed during grinding by the different samples. No significant differences were observed between both studied microstructures. In general, a growing tendency can be noticed as work speed and wheel speed increase, the other variables remaining constant. This trend becomes even more noticeable when wheel speed is changed, since it plays a direct role on the power required. Concurrently, mean undeformed chip thickness decreases, thereby increasing friction and tangential force, the other factor with direct effect on power.

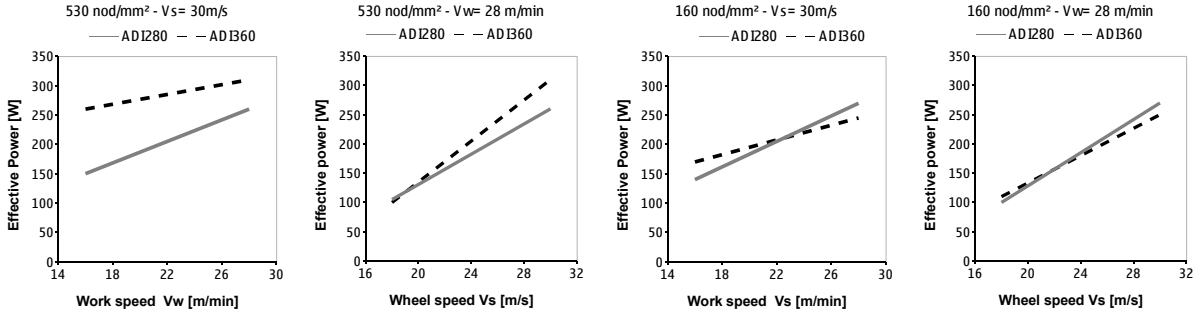

Fig. 3. Effective power consumed during grinding of ADI

3.4 Distortion of ground samples

Table 6 summarizes the distortion values obtained from ground samples. Positive values correspond to concave shape distortion, while negative ones indicate convex shape distortion. As it can be noticed, most assays resulted in concave shape distortion, associated to a tensile residual stress profile, as described by Sosa et al. (2006) and ASM (1996). This kind of profile is generated when temperature gradients in the contact area have greater prominence than stress due to plastic deformations. Under condition (III), distortion reached the highest value, which is related to greater friction and heat produced under said condition. Ground samples under condition (I) yielded lesser distortion, and, hence, lesser residual stress. Under such condition, the amount of material extracted after each abrasive grit was greater, producing greater localized forces which would balance thermal stresses.

Table 6. Distortion of ground samples

			530 nod/mm^2		160 nod/mm^2	
Condition	Vs [m/s]	Vw[m/min]	ADI280	ADI360	ADI280	ADI360
I	20	28	+0.07	+0,07	-0.03	-0.01
II	30	28	+0.08	+0.17	+0.06	+0.07
III	30	16	+0.14	+0.64	+0.26	+0.26

It was noticed that in lower nodule count samples, the distortions produced in ADI280 samples did not differ significantly from those produced in ADI360 samples. Besides, ADI360 samples with 530 nod/mm^2 were subject to greater distortion when being ground at the highest wheel speed (conditions II and III). Such difference became even more significant when the lowest work speed was used (condition III). This behavior is directly related to the increase in friction produced when the mean undeformed chip thickness is decreased. Moreover, the presence of a greater amount of austenite and the more open structure with less interphases and lattice distortion conferred ADI360 samples lower yield strength.

4. Conclusions

Samples of ADI grade 2 and 5, whose hardness values fulfilled ASTM A897 standard, were obtained. Microstructures were metallographically characterized by x-ray diffraction, obtaining the percentage distribution of phases and their features.

ADI surfaces subject to conventional reciprocating surface grinding under semi-rough conditions with a standard vitrified wheel identified as IC36/46I/J5V9 and a 5% aqueous solution soluble oil as cooling fluid showed no surface defects such as burns, laps or cracks.

Surface roughness under operating conditions was lower than expected for finish grinding in low resistance iron-base alloys, yielding very good surface finish.

The power required to perform grinding relies mainly on the operating conditions used, and increasingly grows with wheel speed.

The distortions produced in thin samples denote the generation of a tensile stress profile. The lowest distortions were obtained with low wheel speed and high work speed in the analyzed range. Samples austempered at 360 ºC yielded greater distortion.

References

ASM, 1996. International Handbook Committee, Volume 5 Surface Engineering, ASM International.

Basso A., Sikora J., 2012. Review on production processes and mechanical properties of dual phase austempered ductile iron. International Journal of Metalcasting. 6 (1), 7–14.

Caldera M., Massone J., Boeri R., Sikora J., 2004. Impact properties of thin wall ductile iron. ISIJ International 44 (4), 731–736.

Caldera M., Chapetti M., Massone J. M., Sikora, J. A., 2007. Influence of nodule count on fatigue properties of ferritic thin wall ductile iron. Materials Science and Technology 23 (8), 1000-1004.

David P., Massone J., Boeri R., Sikora J., 2004. Mechanical properties of thin wall ductile iron – Influence of carbon equivalent and graphite distribution. ISIJ International 44 (7), 1180–1187.

Kraus W., Nolze G., 1998. Powder Cell 2.3 version. CPD Newsletter, 20, 274.

Laino S., Sikora J., Dommarco R.C., 2011. Advances in the development of carbidic ADI. Key Engineering Materials 457, 187–192.

Massone J., Boeri R.E., Sikora J. A., 2003. Solid state transformation kinetics of high nodule count ductile iron. International Journal of Cast Metals Research 16 (1-3), 179–184.

Rebasa N., Dommarco R., Sikora J.A., 2002. Wear resistance of high nodule count ductile iron, Wear 253, 855–861.

Sosa A.D., Moncada O.J., Echeverria M.D., Sikora J.A., 2007. Residual stresses, distortion and surface roughness produced by grinding thin wall ductile iron plates. International journal of Machine Tools and Manufacture 47, 229–235.

Sosa A.D., Moncada O.J., Echeverria M.D., Mingolo N., Sikora J.A., 2009. Influence of nodule count on residual stresses and distortion in thin wall ductile iron plates of different matrices. Journal of Materials processing technology 209, 5545–5551.

Sosa A.D, Moncada O.J., Sikora J.A., 2010. Influence of nodule count and other variables on ductile iron decarburization. International Journal of Cast Metals Research 23 (6), 321–329.

Warda R.D., 1990. Ductile Iron Data for Design Engineers. QIT-Fer et Titane INC.